Technical Note

Predictors for Clear-Water and Live-Bed Scour at Circular Piers

Daniel Rebai[1]; Alessio Radice[2]; Francesco Ballio[3]; and Silvio Franzetti[4]

Abstract: In this work, we propose a new predictor for estimating the local scour at circular piers in live-bed conditions, explicitly accounting for the dependence of the time-averaged equilibrium scour depth on dimensionless factors for pier slenderness, sediment coarseness, sediment gradation, and flow intensity. The empirical model is constructed as the product of four independent subfunctions, a modular formulation that simplifies the normalization of experimental data and enables a clear interpretation of the individual effects of these parameters. The presented equation outperforms other approaches proposed in the literature. We also present a full trend of the equilibrium scour depth as a function of the flow intensity for both clear-water and live-bed regimes (for flow velocity up to 4.5 times the threshold for sediment motion in the unobstructed reach). For the estimation of the scour depth in clear-water condition we slightly modified a predictor that we recently proposed. Our formulae are supported by an extensive data set comprising 1,175 experimental data points, underscoring the robustness and applicability of the proposed model. For uniform sediment, the maximum scour occurs in the clear-water regime. By contrast, in flows with nonuniform sediment, the worst-case scenario occurs in the live-bed regime. **DOI: 10.1061/JHEND8.HYENG-14569.**

Introduction

Scour around bridge piers is widely recognized as a critical factor contributing to the failure of waterway bridges globally, with a significant proportion of collapses attributed to sediment removal and resulting foundation instability during high flowrate events (Wardhana and Hadipriono 2003; Melville and Coleman 2000; Richardson and Davis 2001; D'Angelo et al. 2025). The local flow field around a bridge pier is complex: the disruption of the incoming flow creates distinct patterns, including downflow at the pier face and horseshoe vortices. These components govern the formation and progression of scour, as studied in the pioneering work of, for example, Hjorth (1975), Melville (1975), Melville and Raudkivi (1977), and Ettema (1980).

If the bed shear stress upstream of the bridge is lower than the critical value for incipient motion (Shields 1936), sediment transport does not occur. However, even under such conditions, sediment around the pier still can be eroded, a phenomenon known as clear-water scour. Conversely, when the upstream shear stress exceeds the critical value, sediment motion extends in the vicinity of the bridge pier, leading to a process called live-bed scour. In the clear-water regime, the evolution of scour is slow, and the process eventually stabilizes over long timescales (Simarro-Grande and Martín-Vide 2004; Lança et al. 2013). In contrast, live-bed scour evolves more rapidly, and oscillates around a mean equilibrium value (Raudkivi 1986), which is reached when the sediment inflow from upstream balances the sediment removal due to the scour process.

Although semiempirical models (Baker 1980; Kothyari et al. 1992; Dey 1999; Guo 2014), numerical simulations (Olsen and Melaaen 1993; Khosronejad et al. 2012; Olsen and Kjellesvig 1998; Roulund et al. 2005; Cheng et al. 2018), theoretical works based on the phenomenological theory of turbulence (Manes and Brocchini 2015; Coscarella et al. 2020; Ali and Dey 2024; Dey and Ali 2024), and data-driven approaches (Choi et al. 2017; Ebtehaj et al. 2019; Chou and Nguyen 2022; Singh et al. 2022; Pandey et al. 2023) provide valuable tools for describing scour processes, the use of dimensionless coordination of experimental data remains a cornerstone in both research and practical applications. Empirical fitting of dimensionless data is a relatively simple yet effective means of analyzing and predicting complex scour phenomena, facilitating the comparison of results across different experimental setups and conditions. Building on this established foundation, Franzetti et al. (2022) introduced a new predictor for the time-dependent, spatially maximum scour depth at circular piers under clear-water flow conditions. In the present work, we extend the Franzetti et al. (2022) model to live-bed conditions, focusing on the time-averaged equilibrium scour depth, and explicitly accounting for dimensionless factors for pier slenderness, sediment coarseness, sediment gradation, and flow intensity. Finally, we propose two formulae for predicting scour depths across both clear-water and live-bed regimes.

Scour Function

Dimensional Analysis

The time-averaged spatially-maximum equilibrium scour depth (d_s) within the scour hole of a circular pier in equilibrium live-bed condition can be modeled by the following functional relationship:

[1]Research Associate, Institut für Wasser und Umwelt, Karlsruher Institut für Technologie, Kaiserstraße 12, Karlsruhe 76131, Germany; formerly, Postdoctoral, Dept. of Civil and Environmental Engineering, Politecnico di Milano, Piazza L. da Vinci 32, Milano 20133, Italy (corresponding author). ORCID: https://orcid.org/0000-0003-4277-7320. Email: daniel.rebai@kit.edu

[2]Professor, Dept. of Civil and Environmental Engineering, Politecnico di Milano, Piazza L. da Vinci 32, Milano 20133, Italy. ORCID: https://orcid.org/0000-0001-5024-3199. Email: alessio.radice@polimi.it

[3]Professor, Dept. of Civil and Environmental Engineering, Politecnico di Milano, Piazza L. da Vinci 32, Milano 20133, Italy. Email: francesco.ballio@polimi.it

[4]Retired; formerly, Professor, Dept. of Civil and Environmental Engineering, Politecnico di Milano, Piazza L. da Vinci 32, Milano 20133, Italy. Email: silvio.franzetti@polimi.it

Note. This manuscript was submitted on March 14, 2025; approved on September 2, 2025; published online on November 25, 2025. Discussion period open until April 25, 2026; separate discussions must be submitted for individual papers. This technical note is part of the ***Journal of Hydraulic Engineering***, © ASCE, ISSN 0733-9429.

$$d_s = F(\rho, \mu, l_c, h, b, u, d_{50}, \sigma_g, \rho_g, g) \quad (1)$$

where ρ = water density; μ = water viscosity; l_c = channel width; h = water depth; b = pier diameter; u = flow velocity; d_{50} = median sediment size; σ_g = sediment gradation coefficient; ρ_g = sediment density; and g = acceleration due to gravity.

As shown by Franzetti et al. (2022), the dimensionless counterpart of this relationship is

$$D_S = \tilde{F}(\mathrm{R}, B, H, D_{50}, \sigma_g, \Delta, U) \quad (2)$$

where $D_s = d_s/b$ = dimensionless scour depth; $\mathrm{R} = \rho u h/\mu$ = Reynolds number; $B = b/l_c$ = constriction ratio; $H = h/b$ = pier slenderness ratio; $D_{50} = b/d_{50}$ = sediment coarseness ratio; $\Delta = (\rho_g - \rho)/\rho$ = sediment density ratio; and $U = u/u_c$ is a flow intensity parameter, where u_c = threshold velocity for sediment transport in the unobstructed reach upstream of the pier. In the clear water regime, Franzetti et al. (2022) studied the temporal evolution of the scour depth, and therefore included the dimensional (t) and dimensionless ($T = tu/b\Delta^{0.5}$) times in Eqs. (1) and (2), respectively. Moreover, Franzetti et al. (2022) demonstrated that if the critical velocity is included in Eq. (1), the Froude number also will be an independent variable in Eq. (2).

Database

In this study, we analyzed a data set comprising 47 distinct sources, collectively contributing 1,175 experimental data points. Fig. 1 illustrates the characteristics of the entire data set, as well as those of each subset provided by individual researchers. For each author and each variable, a rectangle indicates the experimental range. Each data point is represented by a filled circle: the darker the region, the greater is the concentration of data. The number of experiments reported by each researcher is shown on the right side of the figure.

The critical velocity was computed consistent with the approach used by Franzetti et al. (2022) and according to Lança et al. (2016). For the scour function in the live-bed regime ($U > 1.05$), we considered 20 sources, totaling 473 data points. For the clear-water regime, we included 46 sources, yielding 702 data. Furthermore, we adopted the same methodological framework as in previous analyses, and included only data that met the criteria outlined by Franzetti et al. (2022), specifically a time constraint of $T > 5 \times 10^4$

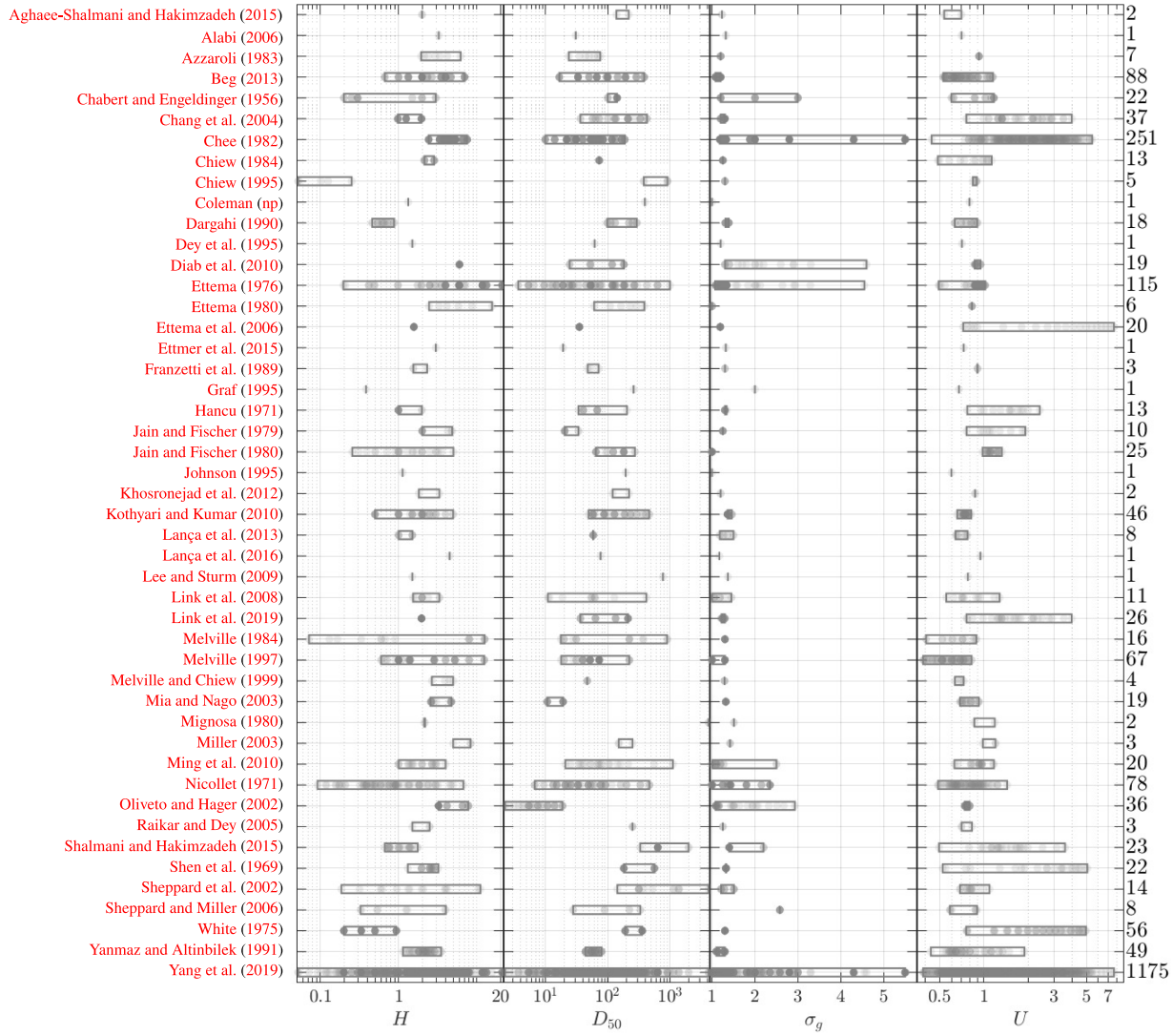

Fig. 1. Characteristics of the data set. For each researcher and variable, the experimental range is depicted by a rectangle, and individual data points are shown as filled circles. Darker regions indicate higher data density. The total number of experiments per researcher is displayed on the right.

(not explicitly shown) and a constriction ratio of $B < 0.125$. Figs. S1 and S2 present the same information separately for clear-water and live-bed data.

Live-Bed Model

Before introducing the scour predictor, we outline several key assumptions underlying the dimensionless functional relationships. Assuming fully turbulent flow, we consider the Reynolds number to be irrelevant. Ballio et al. (2009) demonstrated that when the constriction ratio $B < 0.125$, the influence of B on D_s is negligible (no filter was imposed on B, because it is smaller than 0.125 in 93% of the data set). As shown by Radice et al. (2009), the relative density, Δ, primarily influences the definition of the dimensionless time, and can be excluded by Eq. (2).

In addition to these assumptions, we adopt the hypothesis of separate effects of dimensionless parameters, a framework employed by several researchers in the field (Kothyari et al. 1992; Franzetti et al. 1994; Melville and Coleman 2000; Oliveto and Hager 2002). This hypothesis posits that each parameter exerts an independent influence on the scour process, enabling the development of a predictive model based on the product of individual parameter functions. By invoking this principle, we derive a predictor in the form

$$D_s = aF_1(H)F_2(D_{50})F_3(\sigma_g)F_4(U) \tag{3}$$

where $a = 1.69$, and [keeping the same structure as Franzetti et al. (2022)]

$$F_1(H) = 1 - 0.7513e^{-1.426H} \tag{4a}$$

$$F_2(D_{50}) = 0.318\left(D_{50}^{1.817}e^{-4.491D_{50}^{0.1861}} + 0.205\right) \tag{4b}$$

$$F_3(\sigma_g) = 3.644\left(e^{-2.014\cdot10^{-4}\sigma_g^{7.962}} + 2.644\right) \tag{4c}$$

$$F_4(U) = 1 - 6.006 \times 10^{-3}(1-U)^3 \tag{4d}$$

Fig. 2 provides a comprehensive depiction of the trends in scour depth as a function of the parameters, including pier slenderness [Eq. (4*a*) and Fig. 2(a)], sediment coarseness [Eq. (4*b*) and Fig. 2(b)], sediment gradation coefficient [Eq. (4*c*) and Fig. 2(c)], and flow intensity [Eq. (4*d*) and Fig. 2(d)]. Fig. S3 shows a color version of Fig. 2, using distinct markers and colors for each source. Contrary to other approaches, we do not look for an envelope curve describing the worst-case scenario (Melville 1997), bur rather we extract the best-fit of the data set, as did Franzetti et al. (2022). The validity ranges of the proposed model are $H \in (0.20, 8.33)$, $D_{50} \in (9.43, 4, 154)$, $\sigma_g \in (1, 5.5)$, and $U \in (1.05, 7.68)$.

The scour depth D_S exhibits a direct relationship with the pier slenderness parameter H, increasing steadily as H increases and eventually approaching a horizontal asymptote at approximately $H \approx 3.5$; D_S increases as D_{50} increases, reaching a peak at $D_{50} \approx 70$, after which it begins to decrease. For sediments with a high degree of uniformity, characterized by a sediment gradation index $\sigma_g < 1.3$, the effect of sediment nonuniformity on scour depth is minimal. However, as the sediment gradation index increases above $\sigma_g > 2$, the scour depth begins to decline relative to that for uniform sediments. Beyond a certain threshold, the influence of sediment nonuniformity decreases, and the relationship between scour depth D_S and σ_g approaches a horizontal asymptote $F_3(\sigma_g > 3) = 0.7$. The scour depth also has significant dependence on flow intensity, characterized by the parameter U. For $U > 1$, the function is convex,

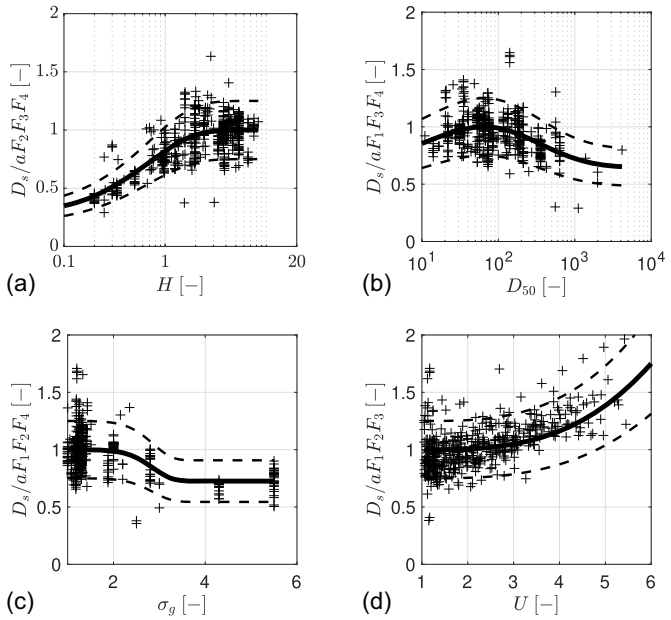

Fig. 2. Scour functions in live-bed: (a) $F_1(H)$; (b) $F_2(D_{50})$; (c) $F_3(\sigma_g)$; and (d) $F_4(U)$. Crosses = data; thick continuous line = scour function; and thin dashed lines = ±25% bounds.

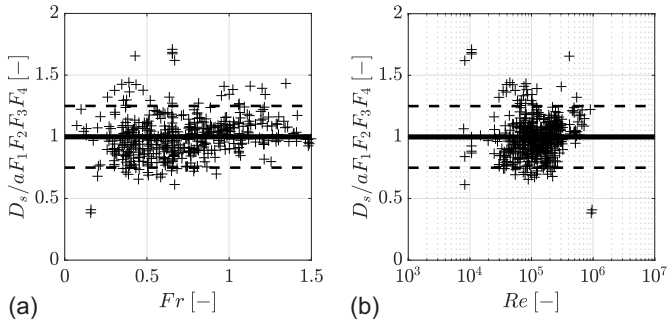

Fig. 3. Measured equilibrium scour depth in live-bed normalized with the predictor $aF_1F_2F_3F_4$ as a function of (a) Froude number, Fr; and (b) Reynolds number, R. Data are shown using crosses. The solid line shows a function equal to one, and the dashed lines represent a ±25% confidence bound.

reflecting an accelerating increase in scour depth with higher flow intensities.

Fig. 3 presents the normalized equilibrium scour depth, $D_s/F_1(H)F_2(D_{50})F_3(\sigma_g)F_4(U)$, as a function of the Froude number [Fig. 3(a)], and Reynolds number [Fig. 3(b)]. The absence of a discernible trend supports the assumption that D_s is independent of these variables. Fig. S4 presents the same plot distinguishing data sources by color.

Discussion

Model Performance

To evaluate the predictive capabilities of our scour function, we compared the measured scour values and those predicted by the model. This comparison is depicted in Fig. 4(a), which plots the measured data versus the values computed using Eqs. (3) and (4).

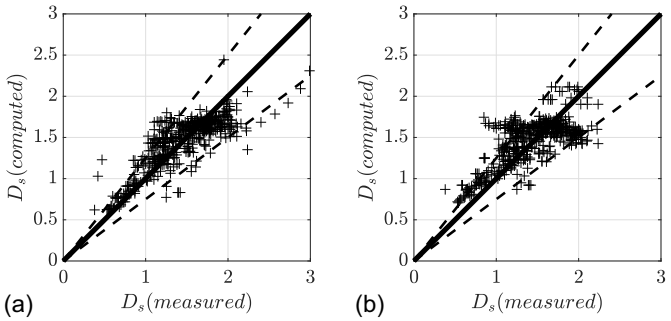

Fig. 4. Computed scour depth value versus the measured scour depth. Data are shown using crosses. The solid curve is the perfect agreement line (slope 1:1), and the dashed lines represent a ±25% confidence bound: (a) this work; and (b) the model proposed by Sheppard et al. (2014).

Table 1. Performance indicators for various formulas in relation to data set used in this manuscript

Reference	Mean	RMS error	NSE	P_{OUT} (%)
This work	0.00	0.24	0.70	11
Sheppard et al. (2014)	−0.03	0.28	0.47	21
Johnson (1995)	−0.28	0.48	−0.56	32
Laursen and Toch (1956)	−0.33	0.49	−0.66	36
Coleman (1971)	0.05	0.40	−0.08	41
Veiga (1970)	−0.33	0.49	−0.66	36
Hancu (1971)	−0.46	0.58	−1.31	50
Fischenich and Landers (1999)	−0.90	1.48	−13.99	54
Laursen (1963)	−0.36	0.66	−1.96	48
Yanmaz and Altinbilek (1991)	−0.90	1.48	−13.99	54
Kothyari et al. (1992)	−0.51	0.67	−2.07	54
Gao et al. (1993)	−0.61	0.80	−3.36	62
Melville and Raudkivi (1977)	−0.71	0.78	−3.16	76
Chitale (1962)	−1.49	3.42	−79.22	87
Froehlich (1988)	0.79	0.84	−3.81	97

The alignment of the data points along the perfect agreement line (solid curve) indicates a high degree of correspondence between the model predictions and the experimental observations. Additionally, a ±25% confidence interval (dashed lines) is included to account for potential uncertainties in the measurements or experimental setup. A total of 89% of the data points were within this range, further demonstrating the reliability of the model.

We also compared the scour predictor proposed in this study with other approaches presented in the literature. Specifically, we considered the formulae reported by Baranwal and Das (2024), with a focus exclusively on equations applicable to the live-bed regime. In line with the approach used by Franzetti et al. (2022), we excluded experiments involving lightweight sediment, because many of the formulae in the literature were developed using natural sediment. Overall, we examined a total of 14 different formulae, which were proposed by the following researchers: Laursen and Toch (1956), Chitale (1962), Laursen (1963), Coleman (1971), Hancu (1971), Melville (1975), Froehlich (1988), Kothyari et al. (1992), Johnson (1995), Gao et al. (1993), Melville (1997), Fischenich and Landers (1999), Yanmaz and Altinbilek (1991), and Sheppard et al. (2014).

Table 1 reports four performance indicators computed for each model: the mean, the RMS error, the Nash–Sutcliffe efficiency (NSE), and the percentage of points outside the ±25% confidence

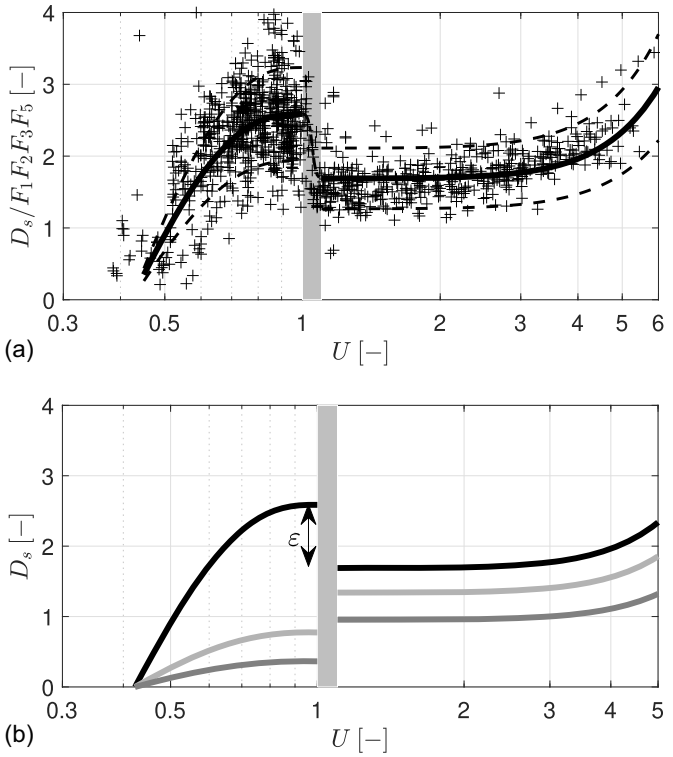

Fig. 5. (a) Scour depth as a function of the flow intensity for clear-water and live-bed condition. Crosses = data; thick continuous line = scour function; and thin dashed lines ±25% bounds; and (b) scour depth versus flow intensity for cases of a laboratory flume with uniform sediments (black), a torrential river (light gray), and an alluvial river (dark gray).

interval. Based on the data presented in Table 1, we conclude that our model provides the best performance among those evaluated in this study. Fig. 4(b) shows the computed scour versus of that predicted by Sheppard et al. (2014), which is the second-best model in Table 1. Fig. S5 depicts the same comparison, distinguishing data sources by color.

Insights into the Effect of Flow Intensity

Fig. 5(a) illustrates the relationship between the scour depth and the flow intensity parameters under both clear-water and live-bed conditions. As was done for Fig. 2, to isolate the effect of U, we divided the measured scour values by the product of the other subfunctions—four in the clear-water regime and three in the live-bed regime, because in the latter we focused solely on the equilibrium scour depth. For $U > 1$, the solid black line corresponds to Eq. (4*d*), which provides a predictive model for this regime. Fig. S6 presents the same trend, distinguishing data sources by color.

In the clear-water regime, Franzetti et al. (2022) analyzed data within the restricted range $U \in [0.7, 1.05]$ to develop a predictor for the maximum scour depth. However, in the present study, we aimed at a more generalized approach by incorporating all available data for $U < 1$. To this end, we derived a new fitting function, $F_4(U)$, which accurately represents the data in Fig. 5(a). The solid line for the clear-water regime corresponds to the function

$$F_4(U) = 1 - 5.2(1 - U)^3 \tag{5}$$

This function is not identical to Eq. (7d) of Franzetti et al. (2022). However, the difference between the two functions is less

J. Hydraul. Eng., 2026, 152(2): 06025016

than 10% for $U \in [0.7, 1.05]$, ensuring consistency with prior analyses while extending applicability to a broader data set. In the clear-water regime, we recommend using the model proposed by Franzetti et al. (2022) for the functions $F_1(H)$, $F_2(D_{50})$, $F_3(D_{\sigma_g})$, and $F_5(T)$, and Eq. (5) for $F_4(U)$. The validity ranges of the clear-water model are the following: $H \in (0.21, 21.05)$, $T \in (5 \times 10^4 - 3.63 \times 10^7)$, $U \in (0.39, 1.05)$, $D_{50} \in (2.25, 4, 159)$, and $\sigma_g \in (1, 5.5)$.

The near-threshold region, specifically $U \in [1, 1.1]$, is characterized by high uncertainty, and is represented as a shaded area in Fig. 5(a). In Fig. 5, just below the threshold condition, the point scatter is centered around 2.5, whereas just above the threshold condition, it is centered around 1.5. For the calibration of our empirical functions, we used two separate data sets: one for the clear-water regime, and one for the live-bed regime. Because the two interpolators follow the point scatter, they also manifest an abrupt change at about $U = 1$.

The complete trend shown in Fig. 5(a) shows that the proposed model exhibits a pattern similar to that described by Melville (1984) and reported in several manuals (Breusers and Raudkivi 1991; Melville and Coleman 2000; Garcia 2008). Specifically, after reaching a peak at $U = 1$, the scour depth decreases with increasing U, then subsequently increases. Melville (1984) suggested the existence of a second plateau under live-bed conditions, whereas Ettmer et al. (2015) proposed a monotonically increasing function. Because we have only limited data for $U > 4.5$, we cannot draw any conclusions regarding the behavior of $F_4(U)$ at high flow intensities.

Insights into the Effect of Sediment Properties

We now turn our attention to the practical application of the proposed model's findings for river engineering. Here, we want to plot the dimensionless scour depth versus the flow velocity and highlight the effect of sediment properties, such as sediment coarseness and gradation. For the sake of simplicity, we assume that the pier slenderness is sufficiently large, such that $F_1(H) = 1$, and that the scour process has reached equilibrium, meaning $F_5(T) = 1$ in the clear-water regime. Eventually we consider uniform sediment, setting $F_3(\sigma_g) = 1$, and we constrain the sediment size to $D_{50} \in [15, 200]$, a range in which $F_2(D_{50}) \approx 1$: these two conditions were met in more than 60% of the experimental conditions analyzed in this study. Under these assumptions, the resulting scour depth predictions are represented by the black line in Fig. 5(b), which provides a reference for comparison with other scenarios.

Building on this baseline, we analyzed two practical river scenarios as illustrative examples: a torrential river, and an alluvial river. For the torrential river, we assumed a pier width of $b = 1$ m and a median sediment diameter of $d_{50} = 0.2$ m. For the alluvial river, we assumed a pier width of $b = 2.5$ m and a much smaller median sediment diameter of $d_{50} = 0.002$ m. These examples reflect a range of typical conditions encountered in river engineering projects. In both cases, we made a further simplification by considering scenarios in which the pier slenderness effects can be neglected. Specifically, when the pier submergence parameter $H > 3$, $F_1(H) \approx 1$, meaning that slenderness has little to no influence on the scour depth. In practical terms, this corresponds to water depths of $h > 3$ m for the torrential river and $h > 7.5$ m for the alluvial river, both of which are realistic and representative of actual river conditions. In addition, in natural rivers, sediment granulometry rarely is uniform. To account for this variability, we set the nonuniformity parameter $\sigma_g = 3$, reflecting a moderately heterogeneous sediment distribution. This adjustment provides a more realistic representation of the sediment conditions commonly encountered in rivers.

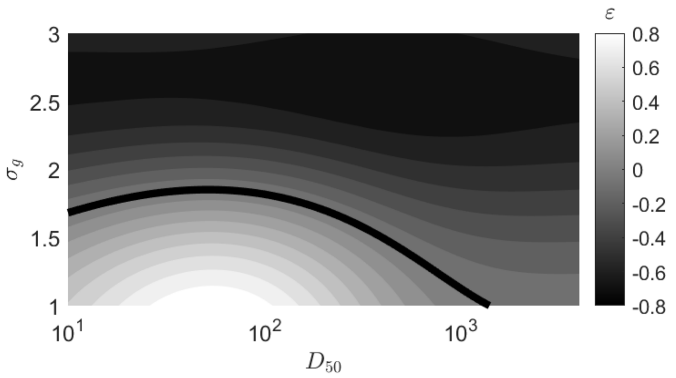

Fig. 6. Colormap of ε as a function of σ_g and D_{50}. The black line represents the condition $\varepsilon = 0$.

Fig. 5(b) presents the scour depth as a function of the flow intensity for both the torrential river (represented by the light gray line) and the alluvial river (represented by the dark gray line). A key observation from these plots is the contrast between curves for uniform and nonuniform sediment. If the sediment is uniform, the clear-water regime typically produces the highest scour values, provided that the flow intensity U remains within moderate ranges. However, this pattern does not hold for nonuniform sediment (which is the standard condition in rivers), for which D_s increases monotonically with increasing values of U. This trend is due to the effect of D_{50} and σ_g on D_s: as the flow condition transitions from clear-water to live-bed, the product $F_2(D_{50})F_3(\sigma_g)$ increased from 0.19 to 0.63 for the torrential river and from 0.14 to 0.57 for the alluvial river. This distinction has significant implications for river engineering design and analysis. Therefore, we recommend adopting the live-bed regime values as a conservative estimate for design and verification purposes: using these values ensures that the designs account for the maximum potential scour depth.

To further substantiate our recommendation, we conducted the following analytical exercise. As in the previous analysis, we assumed that $F_1(H)$ and $F_5(T)$ are equal to unity. Our primary objective was to examine the transition between the two regimes. Therefore, we set $U = 1$ and computed the difference ε between the values of the product $aF_2(D_{50})F_3(\sigma_g)$ under clear-water and live-bed conditions. The resulting variable ε is represented in Fig. 5(b) with reference to the black line. Fig. 6 presents a contour plot of ε in the $\sigma_g - D_{50}$ parameter space, with the black line delineating the boundary at which $\varepsilon = 0$. The sign of ε provides insight into the comparative severity of the two regimes. A positive ε value (light gray in Fig. 6) indicates that clear-water conditions represent the worst-case scenario, whereas a negative ε value (dark gray in Fig. 6) implies that the equilibrium scour depth is greater in the live-bed regime. From this analysis, we conclude that when $\sigma_g > 2$ (a condition frequently observed in natural river systems), the difference ε remains negative regardless of sediment coarseness. This finding indicates that the live-bed condition consistently represents the worst-case scenario under these circumstances.

Additional Recommendations

In the preceding sections, we analyzed the practical applications of our model, particularly in relation to the best-fit estimation of the equilibrium scour depth. Quantification of the dispersion about the mean is necessary whenever safe-side scour evaluations are required. In certain cases, an envelope curve may be preferred over the best-fit method utilized in this study, following an approach

similar to that proposed by Melville (1997). In the clear-water regime, the maximum observed ratio between measured and predicted scour depths was 1.60. Accordingly, by adopting a multiplicative constant of $a = 4.10$, an envelope curve can be established that encompasses all data points. A similar analysis for the live-bed regime yielded a maximum ratio of 1.71, with a recommended constant of $a = 2.89$ for the envelope curve.

Additionally, it is well established that, in the live-bed regime, the scour depth exhibits fluctuations around a quasi-steady equilibrium value. Consequently, considering the maximum scour depth instead of the equilibrium value may be of practical interest. As demonstrated by Radice and Lauva (2017), the amplitude of these scour fluctuations is similar to that of the incoming bed-forms. This finding suggests that the maximum scour depth can be estimated using empirical correlations originally developed for dune height prediction (Gill 1971; Orgis 1974; Raju and Soni 1976; Yalin 1977; Allen 1978; van Rijn 1984).

Furthermore, although circular piers commonly are employed in laboratory experiments, practical applications necessitate consideration of the effects of pier shape and alignment. Although this aspect is beyond the scope of the present study, it is worth noting that such effects can be incorporated into scour prediction models through an additional multiplicative subfunction, as suggested by Melville and Coleman (2000).

Conclusions

This study extends the scour equation proposed by Franzetti et al. (2022) to live-bed flow conditions, providing a versatile framework for predicting the maximum scour depth at circular bridge piers. The proposed model, constructed as the product of four independent subfunctions, effectively incorporates critical parameters, including pier slenderness, sediment coarseness, sediment gradation, and flow intensity. This modular formulation simplifies the normalization of experimental data and provides a clear interpretation of individual parameter effects. Our sensitivity analysis confirmed that the inclusion of additional parameters beyond those considered does not significantly affect scour predictions, enhancing the model's robustness and practical utility. The proposed scour function consistently outperforms existing approaches in the literature, as demonstrated by its ability to match trends across a comprehensive data set comprising 1,1750 experimental data points. The model reveals a significant difference in scour behavior between between cases with uniform and nonuniform sediment. Although the maximum scour occurs under clear-water conditions for uniform sediment in laboratory settings, the worst-case scenario in real rivers with nonuniform sediment arises in the live-bed regime.

Data Availability Statement

Some or all data, models, or code that support the findings of this study are available from the corresponding author upon reasonable request.

Acknowledgments

This study was supported by FABRE (https://www.consorziofabre.it/en/homepage/) through the project "M.Hy.Bridge - Modelling Hydraulic risk at Bridges." This study was carried out within the RETURN Extended Partnership and received funding from the European Union Next-GenerationEU (National Recovery and Resilience Plan—NRRP, Mission 4, Component 2, Investment 1.3—D.D. 1243 2/8/2022, PE0000005). The authors thank Stefania Mirabella, Nicholas Marazzi, and Mary Mansour for contributing to this study during their theses. The authors thank Enrico Busetto Vicari, Costantino Manes, and Francesco Giordana for the fruitful discussion.

Author Contributions

Daniel Rebai: Formal analysis; Writing – original draft; Writing – review and editing. Alessio Radice: Conceptualization; Data curation; Writing – review and editing. Francesco Ballio: Conceptualization; Data curation; Funding acquisition; Writing – review and editing. Silvio Franzetti: Conceptualization; Data curation; Writing – review and editing.

Notation

The following symbols are used in this paper:

a = multiplicative constant of scour predictor;
B = flow constriction ratio ($B = b/l_c$);
b = pier diameter;
D_s = dimensionless scour depth ($D_s = d_s/b$);
D_{50} = sediment coarseness ratio ($D_{50} = b/d_{50}$);
d_s = scour depth;
d_{50} = median sediment size;
Fr = Froude number ($Fr = u/\sqrt{gh}$);
g = acceleration due to gravity;
H = pier slenderness ratio ($H = h/b$);
h = water depth;
l_c = channel width;
P_{out} = percentage of data with more than 25% deviation for predicted D_s;
R = Reynolds number [$\mathrm{R} = (\rho u h)/\mu$];
R_* = shear Reynolds number [$\mathrm{R}_* = (\rho u_* d_{50})/\mu$];
T = dimensionless time [$T = (tu)/(b\Delta^{0.5})$];
t = time;
U = flow intensity ratio ($U = u/u_c$);
u = flow velocity;
u_c = threshold flow velocity for sediment transport;
u^* = shear velocity;
u_c^* = threshold shear velocity for sediment transport;
Δ = sediment density ratio ($\Delta = (\rho_g - \rho)/\rho$);
ε = difference between the values of $aF_2(D_{50})F_3(\sigma_g)$ under clear-water and live-bed conditions at $U = 1$.
θ = Shields number [$\theta = u^{*2}/(g\Delta d_{50})$];
θ_c = threshold Shields number;
μ = water viscosity;
ρ = water density;
ρ_g = sediment density; and
σ_g = sediment gradation coefficient.

Supplemental Materials

Figs. S1–S6 are available online in the ASCE library (www.ascelibrary.org).

References

Aghaee-Shalmani, Y. A., and H. Hakimzadeh. 2015. "Experimental investigation of scour around semi-conical piers under steady current action."

Eur. J. Environ. Civ. Eng. 19 (6): 717–732. https://doi.org/10.1080/19648189.2014.968742.
Alabi, P. D. 2006. "Time development of local scour at a bridge pier fitted with a collar." M.S. thesis, Dept. of Civil and Geological Environmental Engineering, Univ. of Saskatchewan.
Ali, S. Z., and S. Dey. 2024. "Generalized scaling law of equilibrium scour depth at a cylinder embedded in an erodible bed." *Phys. Fluids* 36 (6): 065155. https://doi.org/10.1063/5.0214724.
Allen, J. R. L. 1978. "Computational methods for dune time-lag: Calculations using Stein's rule for dune height." *Sedimentol. Geol.* 20 (3): 165–216. https://doi.org/10.1016/0037-0738(78)90054-4.
Azzaroli, D. 1983. "Analisi sperimentale dell'erosione localizzata attorno ad una coppia di pile inserite in una canaletta di laboratorio." [In Italian.] M.S. thesis, Forestry and Environmental Sciences, Università di Padova.
Baker, C. J. 1980. "Theoretical approach to prediction of local scour around bridge piers." *J. Hydraul. Res.* 18 (1): 1–12. https://doi.org/10.1080/00221688009499564.
Ballio, F., A. Teruzzi, and A. Radice. 2009. "Constriction effects in clear-water scour at abutments." *J. Hydraul. Eng.* 135 (2): 140–145. https://doi.org/10.1061/(ASCE)0733-9429(2009)135:2(140).
Baranwal, A., and B. S. Das. 2024. "Scouring around bridge pier: A comprehensive analysis of scour depth predictive equations for clear-water and live-bed scouring conditions." *Aqua Water Infrastruct. Ecosyst. Soc.* 73 (3): 424–452. https://doi.org/10.2166/aqua.2024.235.
Beg, M. 2013. "Predictive competence of existing bridge pier scour depth predictors." *Eur. Int. J. Sci. Technol.* 2 (1): 161–178.
Breusers, H., and A. Raudkivi. 1991. Vol. 2 of *Scouring: Hydraulic structures design manual series*. 1st ed. Boca Raton, FL: CRC Press.
Chabert, J., and P. Engeldinger. 1956. *Étude des affouillements autour des piles de ponts*. [In French.] Technical report. Chatou, France: Laboratoire National d'Hydraulique.
Chang, W. Y., J. S. Lai, and C. L. Yen. 2004. "Evolution of scour depth at circular bridge piers." *J. Hydraul. Eng.* 130 (9): 905–913. https://doi.org/10.1061/(ASCE)0733-9429(2004)130:9(905).
Chee, R. K. W. 1982. *Live-bed scour at bridge piers*. Rep. No. 290. Auckland, New Zealand: Univ. of Auckland.
Cheng, Z., M. Koken, and G. Constantinescu. 2018. "Approximate methodology to account for effects of coherent structures on sediment entrainment in RANS simulations with a movable bed and applications to pier scour." *Adv. Water Resour.* 120 (Oct): 65–82. https://doi.org/10.1016/j.advwatres.2017.05.019.
Chiew, Y. M. 1984. *Local scour at bridge piers.* Rep. No. 355. Auckland, New Zealand: Univ. of Auckland.
Chiew, Y. M. 1995. "Mechanics of riprap failure at bridge piers." *J. Hydraul. Eng.* 121 (9): 635–643. https://doi.org/10.1061/(ASCE)0733-9429(1995)121:9(635).
Chitale, S. V. 1962. "Scour at bridge crossings." *Trans. Am. Soc. Civ. Eng.* 127 (1): 191–196. https://doi.org/10.1061/TACEAT.0008391.
Choi, S. U., B. Choi, and S. Lee. 2017. "Prediction of local scour around bridge piers using the ANFIS method." *Neural Comput. Appl.* 28 (2): 335–344. https://doi.org/10.1007/s00521-015-2062-1.
Chou, J. S., and N. M. Nguyen. 2022. "Scour depth prediction at bridge piers using metaheuristics-optimized stacking system." *Autom. Constr.* 140 (Aug): 104297. https://doi.org/10.1016/j.autcon.2022.104297.
Coleman, N. L. 1971. "Analyzing laboratory measurements of scour at cylindrical piers in sand beds." In *Proc., 14th Congress of the Int. Association for Hydraulic Research (IAHR)*, 307–313. Madrid, Spain: International Association for Hydraulic Research.
Coscarella, F., R. Gaudio, and C. Manes. 2020. "Near-bed eddy scales and clear-water local scouring around vertical cylinders." *J. Hydraul. Res.* 58 (6): 968–981. https://doi.org/10.1080/00221686.2019.1698668.
D'Angelo, M., M. Civera, P. F. Giordano, P. Borlenghi, F. Ballio, M. P. Limongelli, and B. Chiaia. 2025. "Bridge collapses in Italy across the 21st century: Survey and statistical analysis." *Struct. Infrastruct. Eng.* 1–23. https://doi.org/10.1080/15732479.2025.2483500.
Dargahi, B. 1990. "Controlling mechanism of local scouring." *J. Hydraul. Eng.* 116 (10): 1197–1214. https://doi.org/10.1061/(ASCE)0733-9429(1990)116:10(1197).
Dey, S. 1999. "Time-variation of scour in the vicinity of circular piers." *Proc. Inst. Civ. Eng. Marit. Eng.* 136 (2): 67–75. https://doi.org/10.1680/iwtme.1999.31422.
Dey, S., and S. Z. Ali. 2024. "The universal two-fifths law of pier scour." *Phys. Fluids* 36 (4): 041401.
Dey, S., S. K. Bose, and G. L. N. Sastry. 1995. "Clear water scour at circular piers: A model." *J. Hydraul. Eng.* 121 (12): 869–876. https://doi.org/10.1061/(ASCE)0733-9429(1995)121:12(869).
Diab, R., O. Link, and U. Zanke. 2010. "Geometry of developing and equilibrium scour holes at bridge piers in gravel." *Can. J. Civ. Eng.* 37 (4): 544–552. https://doi.org/10.1139/L09-176.
Ebtehaj, I., H. Bonakdari, A. H. Zaji, and H. Sharafi. 2019. "Sensitivity analysis of parameters affecting scour depth around bridge piers based on the non-tuned, rapid extreme learning machine method." *Neural Comput. Appl.* 31 (12): 9145–9156. https://doi.org/10.1007/s00521-018-3696-6.
Ettema, R. 1976. *Influence of bed gradation on local scour.* Rep. No. 124. Auckland, New Zealand: Univ. of Auckland.
Ettema, R. 1980. *Scour at bridge piers*. Rep. No. 216. Auckland, New Zealand: Univ. of Auckland.
Ettema, R., G. Kirkil, and M. Muste. 2006. "Similitude of large-scale turbulence in experiments on local scour at cylinders." *J. Hydraul. Eng.* 132 (1): 33–40. https://doi.org/10.1061/(ASCE)0733-9429(2006)132:1(33).
Ettmer, B., F. Mueller, and O. Link. 2015. "Live-bed scour at bridge piers in a lightweight polystyrene bed." *J. Hydraul. Eng.* 141 (9): 04015017. https://doi.org/10.1061/(ASCE)HY.1943-7900.0001025.
Fischenich, C., and M. Landers. 1999. *Computing scour: Emrrp technical notes collection (ERDC tn-emrrp-sr-05)*. Technical Rep. Washington, DC: USACE.
Franzetti, S., E. Larcan, and P. Mignosa. 1989. "Erosione alla base di pile circolari di ponte: Verifica sperimentale di esistenza di una situazione di equilibrio." [In Italian.] *Idrotecnica* 3: 135–141.
Franzetti, S., S. Malavasi, and C. Piccinin. 1994. "Sull'erosione alla base delle pile di ponte in acque chiare." [In Italian.] In Vol. T4 of *Proc., 24 Convegno di Idraulica e Costruzioni Idrauliche*, 13–24. Naples, Italy: Istituto di idraulica e costruzioni idrauliche.
Franzetti, S., A. Radice, D. Rebai, and F. Ballio. 2022. "Clear water scour at circular piers: A new formula fitting laboratory data with less than 25% deviation." *J. Hydraul. Eng.* 148 (10): 04022021. https://doi.org/10.1061/(ASCE)HY.1943-7900.0002009.
Froehlich, D. C. 1988. "Abutment scour prediction." In *Proc., 68th TRB Annual Meeting*, Washington, DC: Transportation Research Board.
Gao, D., G. Posada, and C. F. Nordin. 1993. *Pier scour equations used in the People's Republic of China—Review and summary.* Rep. No. FHWA-SA-93076. Washington, DC: US DOT.
Garcia, M. 2008. *Sedimentation Engineering*. Reston, VA: ASCE.
Gill, M. 1971. "Height of sand dunes in open channel flows." *J. Hydraul. Div.* 97 (12): 2067–2074.
Graf, W. 1995. *Load scour around piers*. Rep. No. Lausanne, Switzerland: École Polytechnique Fédérale de Lausanne.
Guo, J. 2014. "Semi-analytical model for temporal clear-water scour at prototype piers." *J. Hydraul. Res.* 52 (3): 366–374. https://doi.org/10.1080/00221686.2013.877527.
Hancu, S. 1971. "Sur le calcul des affouillements locaux dans la zone des piles des ponts." In Vol. 3 of *Proc., 14th IAHR Congress*, 299–313. Delft, Netherlands: International Association for Hydraulic Research.
Hjorth, P. 1975. *Studies on the nature of local scour.* Rep. No. 46. Lund, Sweden: Lund Institute of Technology.
Jain, S. C., and E. E. Fischer. 1979. *Scour around circular piers at high Froude numbers*. FHWARD-79-104. Washington, DC: USDOT.
Jain, S. C., and E. E. Fischer. 1980. "Scour around bridge piers at high flow velocity." *J. Hydraul. Div.* 106 (11): 1827–1842. https://doi.org/10.1061/(ASCE)HY.1943-7900.0002009.
Johnson, P. A. 1995. "Comparison of pier-scour equations using field data." *J. Hydraul. Eng.* 121 (8): 626–629. https://doi.org/10.1061/(ASCE)0733-9429(1995)121:8(626).
Khosronejad, A., S. Kang, and F. Sotiropoulos. 2012. "Experimental and computational investigation of local scour around bridge piers." *Adv. Water Resour.* 37 (Mar): 73–85. https://doi.org/10.1016/j.advwatres.2011.09.013.

Kothyari, U. C., R. C. J. Garde, and K. G. Ranga Raju. 1992. "Temporal variation of scour around circular bridge piers." *J. Hydraul. Eng.* 118 (8): 1091–1106. https://doi.org/10.1061/(ASCE)0733-9429(1992)118:8(1091).

Kothyari, U. C., and A. Kumar. 2010. "Temporal variation of scour around circular bridge piers." Supplement, *ISH J. Hydraul. Eng.* 16 (S1): 35–48. https://doi.org/10.1080/09715010.2012.695452.

Lança, R., C. S. Fael, R. J. Maia, J. P. Pêgo, and A. Cardoso. 2013. "Clear-water scour at comparatively large cylindrical piers." *J. Hydraul. Eng.* 139 (11): 1117–1125. https://doi.org/10.1061/(ASCE)HY.1943-7900.0000788.

Lança, R., G. Simarro, C. M. S. Fael, and A. H. Cardoso. 2016. "Effect of viscosity on the equilibrium scour depth at single cylindrical piers." *J. Hydraul. Eng.* 142 (3): 06015022. https://doi.org/10.1061/(ASCE)HY.1943-7900.0001102.

Laursen, E. M. 1963. "An analysis of relief bridge scour." *J. Hydraul. Div.* 89 (3): 93–118. https://doi.org/10.1061/JYCEAJ.0000896.

Laursen, E. M., and A. Toch. 1956. *Scour around bridge piers and abutments*. Rep. No. Bulletin No. 4. Ames, IA: Iowa Highway Research Board.

Lee, S. O., and T. W. Sturm. 2009. "Effect of sediment size scaling on physical modeling of bridge pier scour." *J. Hydraul. Eng.* 135 (10): 793–802. https://doi.org/10.1061/(ASCE)HY.1943-7900.0000091.

Link, O., S. Henriquez, and B. Ettmer. 2019. "Physical scale modelling of scour around bridge piers." *J. Hydraul. Res.* 57 (2): 227–237. https://doi.org/10.1080/00221686.2018.1475428.

Link, O., F. Pfleger, and U. Zanke. 2008. "Characteristics of developing scour-holes at a sand-embedded cylinder." *Int. J. Sediment Res.* 23 (3): 258–266. https://doi.org/10.1016/S1001-6279(08)60023-2.

Manes, C., and M. Brocchini. 2015. "Local scour around structures and the phenomenology of turbulence." *J. Fluid Mech.* 779 (Sep): 309–324. https://doi.org/10.1017/jfm.2015.389.

Melville, B., and S. Coleman. 2000. *Bridge scour*. Highlands Ranch, CO: Water Resources Publications.

Melville, B. W. 1975. *Local scour at bridge sites*. Rep. No. 117. Auckland, New Zealand: Univ. of Auckland.

Melville, B. W. 1984. "Live-bed scour at bridge piles." *J. Hydraul. Eng.* 110 (9): 1234–1247. https://doi.org/10.1061/(ASCE)0733-9429(1984)110:9(1234).

Melville, B. W. 1997. "Pier and abutment scour: Integrated approach." *J. Hydraul. Eng.* 123 (2): 125–136. https://doi.org/10.1061/(ASCE)0733-9429(1997)123:2(125).

Melville, B. W., and Y. M. Chiew. 1999. "Time scale for local scour at bridge piers." *J. Hydraul. Eng.* 125 (1): 59–65. https://doi.org/10.1061/(ASCE)0733-9429(1999)125:1(59).

Melville, B. W., and A. J. Raudkivi. 1977. "Flow characteristics in local scour at bridge piers." *J. Hydraul. Res.* 15 (4): 373–380. https://doi.org/10.1080/00221687709499641.

Mia, F., and H. Nago. 2003. "Design method of time-dependent local scour at circular bridge pier." *J. Hydraul. Eng.* 129 (6): 420–427. https://doi.org/10.1061/(ASCE)0733-9429(2003)129:6(420).

Mignosa, P. 1980. "Fenomeni di erosione locale alla base delle pile dei ponti." [In Italian.] M.S. thesis, Dept. of Hydraulic and Hydraulic Structure, Politecnico di Milano.

Miller, W. 2003. "Model for the time rate of local sediment scour at a cylindrical structure." Ph.D. thesis, Civil and Coastal Engineering Dept., Univ. of Florida.

Ming, Z., L. Cheng, and Z. Zang. 2010. "Experimental and numerical investigation of local scour around a submerged vertical circular cylinder in steady currents." *Coastal Eng.* 57 (8): 709–721.

Nicollet, S. 1971. *Deformation des lits alluvionnaires—Affouillement autour des piles de pont cylindriques*. Rep. No. HC7043/689. Chatou, France: Laboratoire National d'Hydraulique.

Oliveto, G., and W. H. Hager. 2002. "Temporal evolution of clear-water pier and abutment scour." *J. Hydraul. Eng.* 128 (9): 811. https://doi.org/10.1061/(ASCE)0733-9429(2002)128:9(811).

Olsen, N. R. B., and H. M. Kjellesvig. 1998. "Three-dimensional numerical flow modeling for estimation of maximum local scour depth." *J. Hydraul. Res.* 36 (4): 579–590. https://doi.org/10.1080/00221689809498610.

Olsen, N. R. B., and M. C. Melaaen. 1993. "Three-dimensional calculation of scour around cylinders." *J. Hydraul. Eng.* 119 (9): 1048–1054. https://doi.org/10.1061/(ASCE)0733-9429(1993)119:9(1048).

Orgis, H. 1974. "Geschiebebetrieb und bettbildung." *Österreichische Ingenieur-Zeitschrift* 17 (9): 285–292.

Pandey, M., M. Karbasi, M. Jamei, A. Malik, and J. H. Pu. 2023. "A comprehensive experimental and computational investigation on estimation of scour depth at bridge abutment: Emerging ensemble intelligent systems." *Water Resour. Manage.* 37 (9): 3745–3767. https://doi.org/10.1007/s11269-023-03525-w.

Radice, A., and O. Lauva. 2017. "Live-bed pier scour in a covered flow." *J. Hydraul. Eng.* 143 (10): 06017016. https://doi.org/10.1061/(ASCE)HY.1943-7900.0001359.

Radice, A., G. Porta, and S. Franzetti. 2009. "Analysis of the time-averaged properties of sediment motion in a local scour process." *Water Resour. Res.* 45 (3): W03401. https://doi.org/10.1029/2007WR006754.

Raikar, R. V., and S. Dey. 2005. "Clear-water scour at bridge piers in fine and medium gravel beds." *Can. J. Civ. Eng.* 32 (4): 775–781. https://doi.org/10.1139/l05-022.

Raju, K. R., and J. Soni. 1976. "Geometry of ripples and dunes in alluvial channels." *J. Hydraul. Res.* 14 (3): 241–249. https://doi.org/10.1080/00221687609499671.

Raudkivi, A. J. 1986. "Functional trends of scour at bridge piers." *J. Hydraul. Eng.* 112 (1): 1–13. https://doi.org/10.1061/(ASCE)0733-9429(1986)112:1(1).

Richardson, E. V., and S. R. Davis. 2001. "*Evaluating scour at bridges [fourth edition]*." Report No. FHWA-NHI-01-001. Washington, DC: Federal Highway Administration.

Roulund, A., B. M. Sumer, J. Fredsøe, and J. Michelsen. 2005. "Numerical and experimental investigation of flow and scour around a circular pile." *J. Fluid Mech.* 534 (Jul): 351–401. https://doi.org/10.1017/S0022112005004507.

Shen, H. W., V. R. Schneider, and S. S. Karaki. 1969. "Local scour around bridge piers." *J. Hydraul. Div.* 95 (6): 1919–1940. https://doi.org/10.1061/JYCEAJ.0002197.

Sheppard, D. M., B. Melville, and H. Demir. 2014. "Evaluation of existing equations for local scour at bridge piers." *J. Hydraul. Eng.* 140 (1): 14–23. https://doi.org/10.1061/(ASCE)HY.1943-7900.0000800.

Sheppard, D. M., and W. J. Miller Jr. 2006. "Live-bed local pier scour experiments." *J. Hydraul. Eng.* 132 (7): 635–642. https://doi.org/10.1061/(ASCE)0733-9429(2006)132:7(635).

Sheppard, D. M., M. Odeh, and T. Glasser. 2002. *Clearwater local sediment scour experiments*. Coastal Engineering Technical Rep. No. 131. Gainesville, FL: Univ. of Florida.

Shields, A. F. 1936. "Application of similarity principles and turbulence research to bed-load movement." *Mitt. der Preuss. Versuchsanstalt für Wasserbau und Schiffbau* 26: 5–24.

Simarro-Grande, G., and J. P. Martín-Vide. 2004. "Exponential expression for time evolution in local scour." *J. Hydraul. Res.* 42 (6): 663–665. https://doi.org/10.1080/00221686.2004.9628320.

Singh, U. K., M. Jamei, M. Karbasi, A. Malik, and M. Pandey. 2022. "Application of a modern multi-level ensemble approach for the estimation of critical shear stress in cohesive sediment mixture." *J. Hydrol.* 607 (Apr): 127549. https://doi.org/10.1016/j.jhydrol.2022.127549.

van Rijn, L. C. 1984. "Sediment transport, Part III: Bed forms and alluvial roughness." *J. Hydraul. Eng.* 110 (12): 1733–1754. https://doi.org/10.1061/(ASCE)0733-9429(1984)110:12(1733).

Veiga, L. 1970. "Discussion to shen et al. (1969)." *Proc. ASCE* 96 (8): 1742–1747. https://doi.org/10.1061/JYCEAJ.0002655.

Wardhana, K., and F. C. Hadipriono. 2003. "Analysis of recent bridge failures in the United States." *J. Perform. Constr. Facil.* 17 (3): 144–150. https://doi.org/10.1061/(ASCE)0887-3828(2003)17:3(144).

White, W. R. 1975. "Scour around bridge piers in steep streams." In Vol. 2 of *Proc., 16th IAHR Congress*, 279–284. Delft, Netherlands: International Association for Hydraulic Research.

Yalin, M. 1977. *Mechanics of sediment transport*. Oxford, UK: Pergamon.

Yang, Y., B. W. Melville, D. M. Sheppard, and A. Y. Shamseldin. 2019. "Live-bed scour at wide and long-skewed bridge piers in comparatively shallow water." *J. Hydraul. Eng.* 145 (5): 06019005. https://doi.org/10.1061/(ASCE)HY.1943-7900.0001600.

Yanmaz, A. M., and H. D. Altinbilek. 1991. "Study of time-dependent local scour around bridge piers." *J. Hydraul. Eng.* 117 (10): 1247–1268. https://doi.org/10.1061/(ASCE)0733-9429(1991)117:10(1247).